The 2010 IEEE/RSJ International Conference on
Intelligent Robots and Systems
October 18-22, 2010, Taipei, Taiwan

Steps in trajectory planning and controller design for a hydraulically driven crane with limited sensing

Daniel Ortíz Morales, Pedro La Hera, Uwe Mettin,
Leonid B. Freidovich, Anton S. Shiriaev, Simon Westerberg

Abstract— **In the forest industry, trees are logged and harvested by human-operated hydraulic manipulators. Eventually, these tasks are expected to be automated with optimal performance. However, with todays technology the main problem is implementation. While prototypes may have rich sensing information, real cranes lack certain sensing devices, such as encoders for position sensing. Automating these machines requires unconventional solutions. In this paper, we consider the motion planning problem, which involves a redesign of optimal trajectories, so that open loop control strategies can be applied using feed-forward control signals whenever sensing information is not available.**

Index Terms— **Motion planning, hydraulic manipulator, implementation, open loop control.**

I. INTRODUCTION

The use of automated robots has become one of the major influences in the increase of productivity of some industrial sectors. In recent years, the enlargement of such technology to a broader range of applications, including outdoor environments, has set new challenges to research in robotics. One of these applications is related to the forest industry, which has proved to be challenging due to the difficulty of the process, and specially the handling of the environmental conditions [1]. However, motivated by the economical benefit of their usage, the development of semi-autonomous forestry machines has become of interest for some entities, as it is the case of the Swedish forest industry.

In this sector, there are mainly two types of off-road vehicles: *the harvester*, which fells and delimbs the trees, and cuts the trunk into logs of a predetermined size, and *the forwarder* (see Fig 1), which collects the logs in a tray and carries them to the nearest road for transportation. In the most usual scenario, each vehicle is equipped with a similar hydraulic manipulator, and the end effector varies according to the process to be performed. Supported by the manufacturers and forestry companies, our group has been working towards the automation of such cranes. The focus of research covers a wide range of problems, and includes tasks such as: modeling, optimal motion/trajectory planning, efficient motion/trajectory representation, controller design, workspace modeling and 3D-reconstruction for tele-operation, human machine interface (HMI) and additional instrumentation for prototyping.

Recently, various scenarios of controlling manipulation tasks were reported [2], [4], [6], in which the problem of planning time-optimal motions and controller design are discussed. These automated motions are intended to provide great assistance and stress relaxation to human drivers. The experimental verification of such work was carried out in a forwarder crane, which is equipped with various sensing devices for pressures and positions to realize feedback control (see Fig. 1). However, it has become clear that most of this development might have a limited value for commercialization, since some variables in the process are unlikely to be measured during real operation. This is the case of links displacement sensing, which inclusion would require serious decisions in redesigning cranes, and which manufacturers are not ready to make. Hence, developing scenarios for (semi)-automated manipulation tasks should be narrowed down to meet constraints imposed on a set of measurement devices reliable for long-time operation, i.e. pressure sensors.

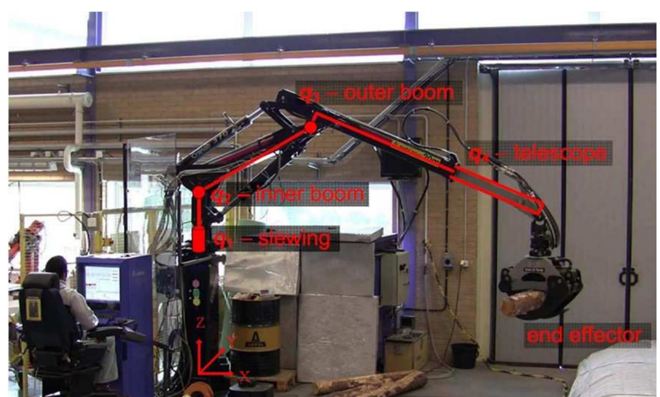

Fig. 1. Laboratory crane installed at the Department of Applied Physics and Electronics, Umeå University. The manipulator is kinematic redundant to the end effector position in the workspace.

The goal of this article is to provide a discussion of preliminary results to the problem of automation of hydraulic manipulators restricted to a limited number of sensing devices. Based on the work reported in [2], [4], we aim at providing complementary steps in motion planning, useful to define a family of motions which execution does not rely

The authors are with the Department of Applied Physics and Electronics, Umeå University, SE-901 87 Umeå, Sweden. E-mail: daniel.ortiz.morales@tfe.umu.se.

A. Shiriaev and U. Mettin are also with the Department of Engineering Cybernetics, Norwegian University of Science and Technology, NO-7491 Trondheim, Norway.

This work is supported by the Center of Intelligent Off-road Vehicles (IFOR) at the Institute of Technology of Umeå University, Komatsu Forest AB, Sveaskog and the Kempe Foundation.

on feedback control. In addition, since angular positions are not measured, a preliminary idea of position estimation based on pressure sensors is presented.

II. Problem formulation

Semi-autonomous motions refers to those trajectories planned to execute parts of a task, reducing in this form the involvement of the driver. Working with a limited number of sensors implies that closed-loop control for stabilization of these motions is not feasible with position as feedback. However, with the knowledge of nominal input signal along a predefined path, a feed-forward open-loop strategy can be sufficient to execute the motion. These open loop signals can be either computed from a model of the system, or measured when all ideal conditions are satisfied, i.e. from a fully instrumented prototyping machine.

The main problem to be found when considering open-loop control is referred to as *divergence*. This implies that when links trajectories are not carefully planned, the resulting motion tends to deviate from the nominal one. The cause of this problem is attributed to the sensitivity of the motion to initial conditions and internal dynamics. However, there is the hypothesis that some finite-time trajectories are less sensitive than others, and can be accurately and repeatably reproduced without active presence of position feedbacks. If initialized wrongly, these family of trajectories remain in a vicinity of the nominal one, i.e. asymptotically stable.

In the following sections we illustrate how such trajectories can be found, and present results of experimental validation to these arguments. In doing so we will

- use as a background standard tools for path constrained trajectory planning,
- extend these methods for taking into account velocity constraints of the hydraulic actuators,
- explain and experimentally validate steps in using pressure measurements for reconstruction of links positions.

III. Kinematic Model

The manipulator used for our study is a downsized version of a typical forwarder crane (see Fig. 1). The kinematic configuration and operational principles are similar to real on-production cranes. It is hydraulically powered and consists of an open kinematic chain of four links from the base to the joint where the end effector is attached. The joints are structured as follows:

(0) Base of the robot manipulator.
(1) Revolute joint for *slewing*, associated with q_1.
(2) Revolute joint for the *inner boom*, associated with q_2.
(3) Revolute joint for the *outer boom*, associated with q_3.
(4) Prismatic joint for *telescopic extension of the outer boom*, associated with q_4.
(5) Joint where end effector is attached (*boom tip*).

The vector of generalized coordinates is defined as $q = [q_1, q_2, q_3, q_4]^T$. The forward kinematics can be conveniently expressed using the Denavit-Hartenberg (DH) convention [5], where each link configuration is represented by the homogeneous transformation

$$A_i = \text{Rot}_{z,\theta_i}\, \text{Trans}_{z,d_i}\, \text{Trans}_{x,a_i}\, \text{Rot}_{x,\alpha_i}\,, \qquad (1)$$

parameterized by joint angle θ_i, link offset d_i, link length a_i, and link twist α_i. In Table I the parameters are provided describing the configuration of the forwarder crane used in this study.

TABLE I
DH parameters of the 4-link manipulator

Link i	θ_i [rad]	d_i [m]	a_i [m]	α_i [rad]
1	$q_1(t)$	2.202	0	$\pi/2$
2	$q_2(t) + \theta_{2,0}$	0	1.4	0
3	$\pi/2 + q_3(t) - \theta_{2,0}$	0	0.104	$\pi/2$
4	0	$d_{4,0} + q_4(t)$	0	$-\pi/2$
Constants: $\theta_{2,0} = 0.1192\,\text{rad}$, $d_{4,0} = 1.813\,\text{m}$				

Eventually, the Cartesian position of the boom tip with respect to the base frame of the robot is defined by

$$p^0 = \begin{bmatrix} x \\ y \\ z \end{bmatrix} = \begin{bmatrix} I_{3\times3} & 0_{3\times1} \end{bmatrix} T_4^0 \begin{bmatrix} 0_{3\times1} \\ 1 \end{bmatrix} \qquad (2)$$
$$\text{where} \quad T_4^0 = A_1(q_1)A_2(q_2)A_3(q_3)A_4(q_4)\,.$$

The inverse kinematics can be found as a solution of a set of nonlinear trigonometric equations given by T_4^0 in (2). These computations allow to find the vector $[q_1, q_2, q_3]^T$ as function of the cartesian coordinate p^0 and the telescopic extension q_4, i.e.

$$q = F(p^0, q_4). \qquad (3)$$

The configuration and velocity constraints are given in Table II, and they are experimentally found.

TABLE II
Position and velocity constraints of the 4-link manipulator

Link i	$q_{i,\min}$	$q_{i,\max}$	$\dot q_{i,\min}$	$\dot q_{i,\max}$
1	-1	0.5	-0.4	0.4
2	-0.45	1.37	-0.16	0.21
3	-2.7	-0.1	-0.43	0.39
4	0	1.55	-0.67	0.5

IV. Motion planning

In this section the initial steps in motion planning are presented. To this end, the approach of path constrained trajectory planning [3], [4] is applied to design time-optimal motions that regard of velocity constraints. The main principle is to avoid a time-dependence search by introducing parametric descriptions of a path, e.g. time-independent polynomial or trigonometric functions. In this form, motion planning is reduced to the problem of searching for a parametric variable that describes the evolution of the motion. As an illustrative example we consider the following paths:

1) Circular path: This path describes a 2D circle in the x-z–plane of the base frame as depicted in Fig. 2. This unusual path is very illustrative for the analysis of sensitivity of a motion in the vicinity of a nominal one, whenever open loop feed-forward control is used. A parametric description of the motion can be given in the following form

$$p^0(\theta) = \begin{bmatrix} x(\theta) \\ 0 \\ z(\theta) \end{bmatrix} = \begin{bmatrix} R \cdot \cos(\theta) \\ 0 \\ R \cdot \sin(\theta) \end{bmatrix} + \begin{bmatrix} x_C \\ 0 \\ z_C \end{bmatrix}, \tag{4}$$

where $R = 0.7\,\text{m}$, $[x_C,\, z_C] = [3,\, 2.5]\,\text{m}$ and $\theta \in [-\pi,\, \pi]$

In these equations, the arc length along the path is a choice that naturally yields a monotonic evolution, and can be calculated as follows

$$\theta = \operatorname{atan2}(z - z_C,\, x - x_C)\,. \tag{5}$$

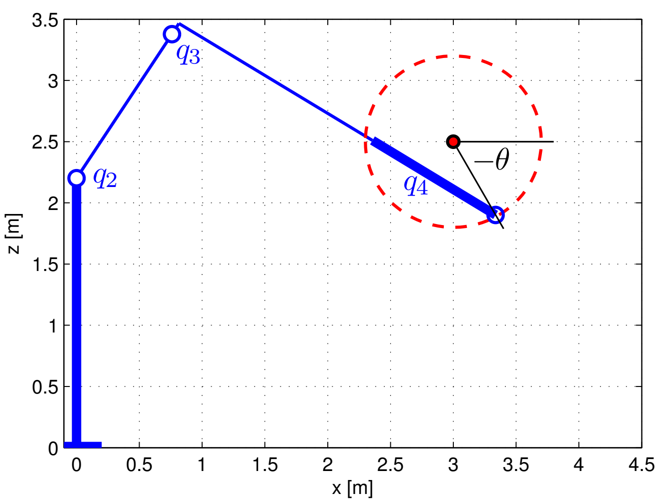

Fig. 2. Path of the boom tip describing a 2D circle in the x-z–plane of the base frame.

2) Parabolic path: This path is a 3D parabola similar to those performed for logging (see Fig. 3). A parametric description of the path can be given as function of the monotonic movement in the x-direction, i.e.

$$\theta = x\,, \tag{6}$$

which allows to define

$$p^0(\theta) = \begin{bmatrix} x(\theta) \\ y(\theta) \\ z(\theta) \end{bmatrix} = \begin{bmatrix} \theta \\ \tan(\alpha) \cdot \theta \\ \frac{(\theta+h)^2}{4 \cdot a} \end{bmatrix} + \begin{bmatrix} 0 \\ 0 \\ k \end{bmatrix},$$

$$\text{where } \alpha = -\tfrac{\pi}{3}\,\text{rad}, \quad \theta \in [x_0,\, x_{end}] = [1.6, 3.07]\text{m}, \quad [h,\, k] = [\tfrac{x_0 + x_{end}}{2},\, z_{max}], \quad [z_{min}, z_{max}] = [1.5,\, 3]\,\text{m}. \tag{7}$$

Since the vertex must be the maximum of the parabola $a < 0$. The distance between the vertex to the directrix is computed by

$$a = \frac{(x_0 - h)^2}{4(z_{min} - k)}. \tag{8}$$

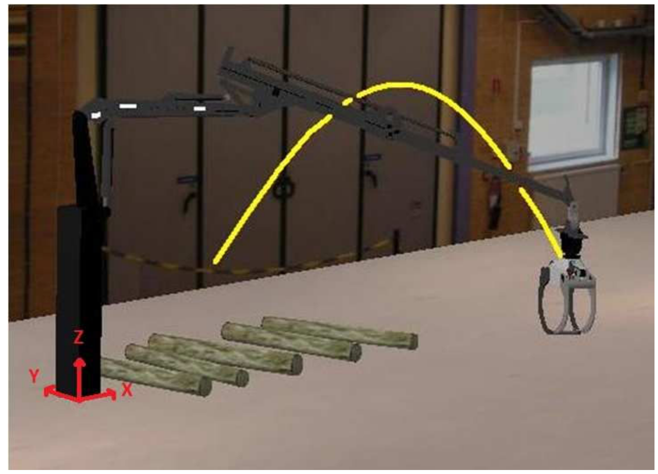

Fig. 3. Path of the boom tip describing a 3D parabola in the x-y-z–workspace of the base frame.

A. Path-Constrained Trajectory Planning

Considering the inverse kinematic model (3), a parametric description of the non-redundant degrees of freedom is given by

$$\begin{bmatrix} q_1 \\ q_2 \\ q_3 \end{bmatrix} = \Phi(p^0(\theta), q_4(\theta)) = \Phi(p^0(\theta), \phi_4(\theta)) = \begin{bmatrix} \phi_1(\theta) \\ \phi_2(\theta) \\ \phi_3(\theta) \end{bmatrix}, \tag{9}$$

such that the motion is specified by the evolution of the independent variable θ. With such representation the explicit dependence of time disappears, and $\theta(t)$ becomes the motion generator. In addition, given $\dot{\theta}$ and the function $\phi_4(\theta)$ for the telescopic link, the joint velocities are directly assigned by

$$\dot{q} = \Phi'(\theta)\dot{\theta}\,, \tag{10}$$

such that the full state space vector $[q, \dot{q}]^T$ is parameterized along the path by a proper choice of $[\theta, \dot{\theta}]$ and $\phi_4(\theta)$.

The inclusion of differential constraints in the design of a motion consists in mapping

$$\dot{\theta}_{i,\max}(\theta) = \max\left(\frac{\dot{q}_{i,\max}}{\phi_i'(\theta)}, \frac{\dot{q}_{i,\min}}{\phi_i'(\theta)}\right), \quad i = 1, 2, 3, 4, \tag{11}$$

from (10), into the phase-space $[\theta, \dot{\theta}]$. The maximum and minimum values for these velocities are given in table II. An interpretation of this mapping can be done graphically in the phase-space of $[\theta, \dot{\theta}]$. As shown in Fig. 4, the dark area represents the region to be avoided to properly respect differential constraints. Shaping the region below this dark area by some function, i.e.

$$\dot{\theta} = f(\theta), \tag{12}$$

the solution θ is found by solving the integral:

$$\theta(t) = \int_0^T f(\theta)dt, \tag{13}$$

for the boundary region defined by the parametric variable θ, and given within the time interval $t \in [0, T]$. As a result, the whole motion of the manipulator along a specified path can be generated by following these numerical steps.

B. Time-Efficient Trajectory

To minimize time as performance index, i.e. motion at maximum velocity, implies that the function (12) is shaped closely to the boundaries of the velocity constraints (11). To exemplify this, we consider the paths given by (4, 7), and follow the next procedure:

- Parametrize the redundant joint variable $q_4 := \phi_4(\theta)$ by some function. In the case of the circular path (4), since the motion is periodic, the chosen function is a truncated Fourier Series of order M

$$\phi_4(\theta) = \phi_{40} + \sum_{i=1}^{M} \left(\phi_{4a,i}\cos(i\theta) + \phi_{4b,i}\sin(i\theta)\right) , \quad (14)$$

  while in the parabolic path we selected a Bezier Polynomial of order N.

$$\phi_k(\theta) = \sum_{i=0}^{N} \begin{pmatrix} N \\ i \end{pmatrix} (1-\theta)^{N-i} (\theta)^i P_i, \quad (15)$$

  for this case $k = 4$.
- Apply inverse kinematics (3) to compute the full vector function $\Phi(\theta)$ along the given path.
- The optimal velocity joint profile (14, 15) is found for the coefficients ϕ_{40}, $\phi_{4a,i}$, $\phi_{4b,i}$, P_i that maximize the area under the envelope function formed by the individual joint velocity constraints along the path using (10). A time-efficient trajectory is finally obtained by constructing a smooth curve in the $(\theta, \dot{\theta})$-phase-plane, we took the 90% of the lowest value in upper limits of velocity constraints (11) as the initial and ending points.

The results of this procedure for both examples are shown in Fig. 4.

V. Motion Re-planning for Open Loop Control

As mentioned earlier, the nominal input signals can be found by recording the tracking of the desired trajectories in closed loop. The trajectories found in the previous section can be used for this purpose. However, it is worth to point out that in order to reproduce the motion by open-loop control, all conditions of the closed-loop should be satisfied. This involves the robot initial configuration, links velocities and accelerations. Since in real scenarios the crane is manually driven to the proximity of the initial configuration, the difficulty consists of satisfying initial velocities and accelerations. Therefore, in order to match these circumstances, a redesign of the trajectories has to be made, such that the input signal information allows the motion to start from rest. This scenario is discussed in this section.

The velocity profile is redesign, so that it starts from rest and smoothly connects to the original one as it is shown in Fig. 4. In the case of the circular path after the original velocity profile is reached it will remain in a cycle. In the case of the parabola the idea is to start and end from rest. The intersection points of the velocity profile are selected by

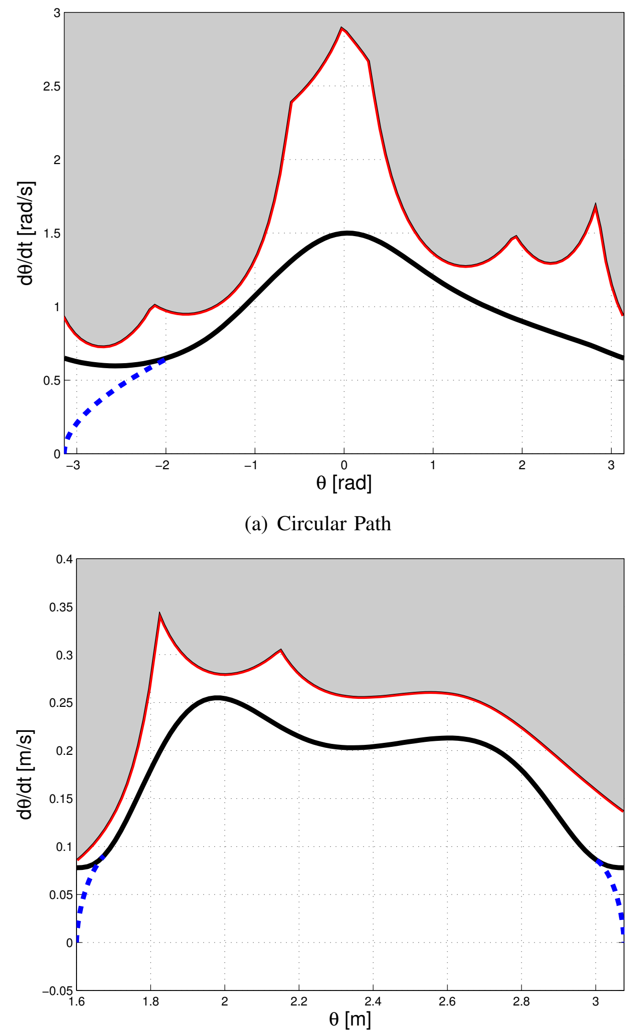

(a) Circular Path

(b) Parabolic Path

Fig. 4. Trajectory in the phase space. The shaded area represent the velocity contraints, the red line is the envelope function which represent the physical limits in velocity, and the black line is the selected joint profile for each path, the blue dashed line is the transition from/to rest to/from the joint profile

$$\theta_{int} = \begin{cases} inf(\theta) + 0.05 * span(\theta) & \text{to start} \\ inf(\theta) + 0.95 * span(\theta) & \text{to end} \end{cases} \quad (16)$$

knowing the intersection points (16) in the velocity profile, from (13) we obtain the required time in the original velocity profile to those intersection points, with these times and by the fact that there are six constraints that must be satisfied, a pair for position, velocity, and acceleration. Then we need to find the coefficients of a fifth order polynomial

$$\theta_{int}(t) = \sum_{i=0}^{5} \left(a_i * t^i_{\theta_{int}}\right) \quad (17)$$

VI. Position Estimation Based on Pressure Sensors

Pressure sensors cannot be used for position feedback, since in principle pressure and position are related by dynamics of the process, and they are difficult to accurately model [2]. Nevertheless, pressure can be used to estimate the position of each link provided our input signal keeps the motion in a vicinity of a particular planned one. To this end, and taking as example the parabolic function (7), we suggest the following procedure.

- By measuring the two chambers A and B of the hydraulic cylinder, we can compute the differential of pressure, which is defined by:

$$\begin{array}{c} \Delta P_i = P_{Ai} - P_{Bi} \\ i = 1, 2, 3, 4 \end{array} \tag{18}$$

- Choose one of the differential of pressures, or a combination of differential of pressures, such that the resulting function is monotonic. In our case the differential of pressure for the first link q_2 shows a monotonic behavior (see Fig. 5). This differential of pressure can be used as a new variable θ to parameterize all joint variables (9).
- Define a polynomial function of the form (15), such that all positions are parametrically defined in terms of the new variable, i.e the differential of pressure (see Fig. 5).

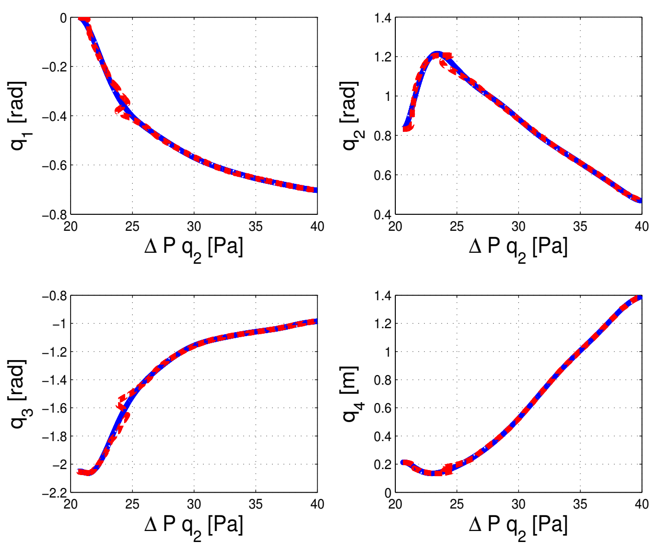

Fig. 5. Parabolic Path: estimation of position for each link with respect to the differential of pressure of the first link, the red dashed line represent the real position and the blue solid line is the estimated position.

Whenever the trajectory is kept in a vicinity of the nominal motion, these polynomials will provide us with an estimation of the position for each of the links with respect to the differential of pressure.

VII. Experimental Results

A. Performance under open loop control

To carry on experimental studies, the prototyping crane depicted in Fig. 1 is employed. This laboratory crane is equipped with various sensing devices and a user interface to monitor the crane behavior. The software used for the implementation of algorithms is Matlab/Simulink.

In order to test the motion performance, we start by analyzing the circular path presented in Fig. 6. To realize this motion, only the nominal input signal is applied to the links. The crane is positioned at the nominal initial condition. After one revolution the drifting becomes clear; however, it is not exponential and it remains in a vicinity of the nominal one. In opposite, if the velocity profile is not redesign to start from rest, the motion diverges immediately from the prescribed one.

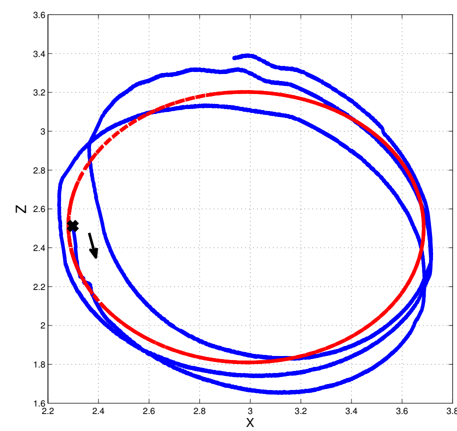

Fig. 6. Circular path in open loop, the red dashed line is the desired trajectory, the blue line is the trajectory in open loop. The initial condition is represented by an X and the arrow shows the direction of the motion

Similarly, for the parabolic path comparable results are obtained. As seen in Fig. 7a, the trajectories for each link in open loop remain closely to the nominal ones. A small deviation is visualized, but for the purpose of the motion it is almost negligible.

B. Performance with mismatch of initial conditions

To test the behavior of the crane under mismatch of initial conditions, we drive the crane to different initial configurations, but in a vicinity to the nominal one. In Fig. 7b it is seen that despite this variation, the trajectories stay in a vicinity defined by an envelope estimated experimentally.

C. Position Estimation

For the case of the parabolic path, the estimation of links positions is shown in Fig. 8 and 5. It is worth to point out that this method is valid only for the constrained trajectories presented, otherwise we can have a set of positions for the same differential of pressure.

VIII. Conclusions

The analysis of different drivers recorded motions reveals that the task of logging is composed by a short number of specific trajectories. These trajectories, which are repeatedly executed throughout the work day, could be introduced in a semi-autonomous way to reduce the work load of the drivers. Interestingly, complex control systems and the introduction of various sensing devices seem to be avoidable, whenever

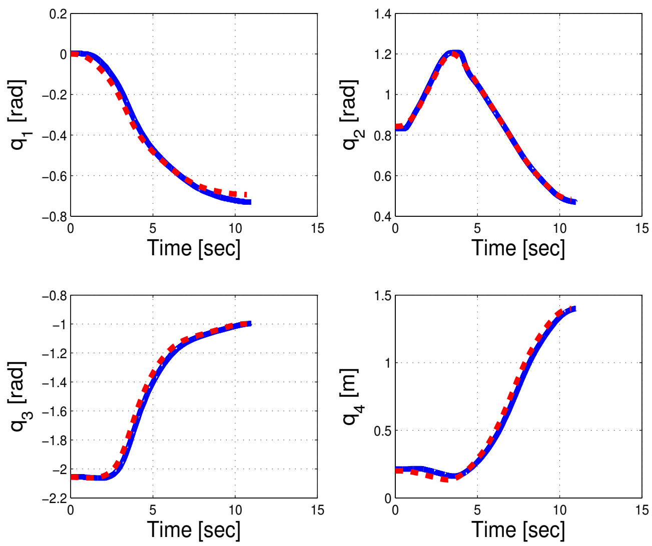

(a) Same initial conditions

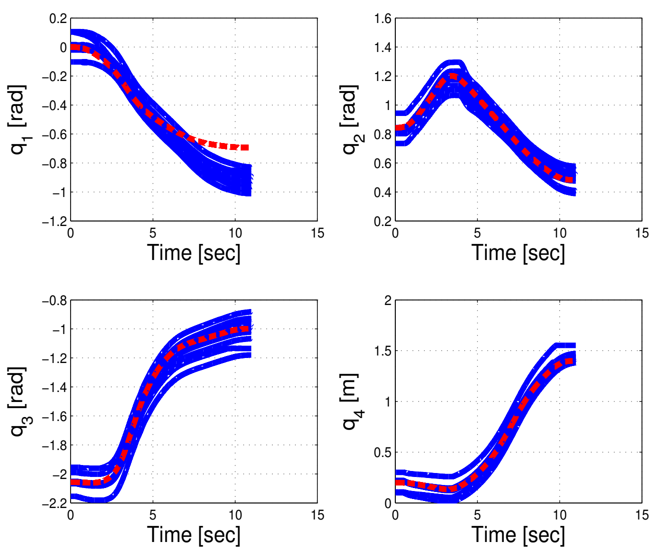

(b) Varying initial conditions for position

Fig. 7. Open Loop Joint Profile Parabolic Path. a) The red dash line is the desired trajectory of each link, the blue line is the trajectory in open loop. b) Similarly, the red dash line is the desired trajectory, and the blue lines are the open loop trajectories with different initial conditions.

careful analysis is used to plan these motions. The work presented here has supported this concept, and motivates that the combination of motion planning and feed-forward open loop control could be perhaps sufficient to accomplish this task.

In order to achieve these results we have presented a procedure for trajectory planning, in which the path is defined in terms of a parametric variable. This method, which is known as path constrained trajectory planning, is used as the basis to define motions that can be re-planned to achieve open loop control. The re-planning of the motion consists of modifying the original trajectories, so to start from rest. In this form, initial conditions of a real operational scenario can be met.

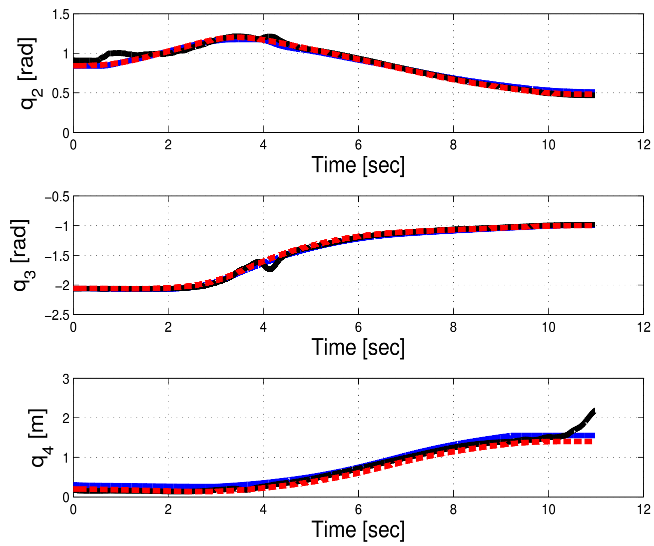

Fig. 8. Parabolic path: estimation of position using pressure sensors, the red dash line is the desired trajectory, the blue line is the real position measured with encoders, the black line is the position estimation

For feed-forward open loop control, the nominal input signals are found by tracking the nominal trajectories in closed loop. This procedure, which is done once for each motion, allows to define a data base in which motion is accompanied by input signal information. Whenever started at the correct initial crane configuration, or in a close vicinity of it, these nominal input signals allow the system to remain within a neighborhood of the planned trajectory.

Due to the absence of position sensing, the links angular movement is estimated by pressure measurements. To this end, the differential of pressure of each link cylinder is computed, with the aim of defining a new monotonic function. By means of this procedure, each link trajectory is parametrically defined as function of this new variable to impose a geometrical relation among them. Noticeably, this estimation is restricted to a specific path.

Experimental results were shown in which these ideas are validated

References

[1] J. Billingsley, A. Visala, and M. Dunn, *Springer Handbook of Robotics*. Berlin Heidelberg: Springer-Verlag, 2008, ch. Robotics in Agriculture and Forestry, pp. 1065–1077.

[2] P. La Hera, U. Mettin, I. Manchester, and A. Shiriaev, “Identification and control of a hydraulic forestry crane,” in *Proceedings of the 17th IFAC World Congress*, Seoul, Korea, July 6-11 2008, pp. 2306–2311.

[3] S. LaValle, *Planning Algorithms*. New York: Cambridge University Press, 2006.

[4] U. Mettin, P. La Hera, D. O. Morales, L. Freidovich, A. Shiriaev, and S. Westerberg, “Trajectory planning and time-independent motion control for a kinematically redundant hydraulic manipulator,” in *Proceedings of the 14th International Conference on Advanced Robotics*, Munich, Germany, Jun. 22-26 2009.

[5] M. Spong, S. Hutchinson, and M. Vidyasagar, *Robot Modeling and Control*. New Jersey: John Wiley and Sons, 2006.

[6] S. Westerberg, I. Manchester, U. Mettin, P. La Hera, and A. Shiriaev, “Virtual environment teleoperation of a hydraulic forestry crane,” in *Proceedings of the 2008 IEEE International Conference on Robotics and Automation*, Pasadena, USA, May 19-23 2008, pp. 4049–4054.